

# Polyelectrolyte adsorption onto an initially-bare solid surface of opposite electrical charge

Svetlana A. Sukhishvili and Steve Granick

*Department of Materials Science and Engineering, University of Illinois, Urbana, Illinois 61801*

(Received 7 April 1998; accepted 24 July 1998)

We contrast the adsorption, over a wide range of  $pH$  and ionic strength, of polyelectrolyte chains with different fractions of charged segments but similar degree of polymerization. The system was a cationic polymer, poly(1,4 vinyl)pyridine (PVP), with 14%, 48%, and 98% quaternized repeat units, adsorbed from aqueous solution ( $D_2O$  or  $H_2O$ ) onto a single silicon oxide substrate at 25 °C. Measurements were based on Fourier transform infrared spectroscopy in attenuated total reflection (FTIR-ATR). In the first phase of this study, we varied the surface charge density by changing  $pH$  and showed that attraction of PVP to the surface was electrostatic. The amount adsorbed of charged (quaternized) PVP segments was nearly the same regardless of the overall fraction of charged segments in the chain. In addition, polymer adsorption appeared to enhance the dissociation of silanol groups on the solid surface. In a second phase of this study, the ionic strength was varied systematically under conditions of high negative surface charge density (high  $pH$ ), focusing on 98% quaternized PVP. Strong chemical specificity was found; the polyelectrolyte was insoluble in KI above a low salt concentration, but soluble in NaCl, signifying that the anions,  $Cl^-$  and  $I^-$ , competed with the negatively-charged surface for association with the polyelectrolyte. At the same time, the cations,  $Na^+$  and  $K^+$ , competed with the polyelectrolyte for access to the limited surface area. The mass adsorbed increased strongly with increasing salt concentration and, for polymer in aqueous NaCl, passed through a maximum with subsequent decrease, reflecting a greater abundance of loops and tails at intermediate ionic strength and ultimately complete desorption of the chains when the salt concentration was very high. The maximum in mass adsorbed occurred at very high ionic strength (1 molar NaCl), indicating competitive adsorption of  $Na^+$  with charged segments of the polymer. Direct measurements of the infrared dichroism of pyridinium rings of the adsorbed PVP confirmed the presence of a relatively flattened state at low ionic strength and nearly isotropic orientation otherwise. In the third phase of this study, we studied the competitive adsorption to surfaces of high negative charge of  $Na^+$  and a monomeric analog of the PVP repeat unit, the 1,4-dimethylpyridinium ion ( $P^+$ ). A tentative quantitative estimate of the effective surface sticking energy of  $P^+$  relative to  $Na^+$  ions indicated a decrease from  $7k_B T$  in low-ionic-strength buffer solution to  $4.5k_B T$  in 0.5 M NaCl. These numbers appear to exceed the weak-adsorption limit in which facile equilibration of the adsorbed layer should be expected. © 1998 American Institute of Physics. [S0021-9606(98)51840-5]

## I. INTRODUCTION

What physical picture should one imagine of flexible polyelectrolytes—flexible polymer chains carrying charged or ionized groups—when they are located at a charged adsorbing surface? It has long been known that for multiple chain adsorption the mass adsorbed usually amounts to more than a monolayer of repeat units. Therefore presumably the segments of chains between adsorption sites loop into solution. Much theoretical attention has been given to equilibrium features of these systems—to describing the spatial distribution of repeat units and especially their electrostatic interactions. Tails at the ends of the macromolecules dangle far into solution; loops of various sizes also dangle into solution; and the entire structure is anchored to the surface by only a fraction of potential adsorption sites. Theoretical models of these configurations have seen much development.<sup>1-7</sup> There are a number of recent reviews of what occurs, or is predicted to occur, at static equilibrium.<sup>8,9</sup> But on the experimental side, information of a definitive quantitative nature

has been difficult to obtain because of the extremely low mass of an adsorbed layer, typically only 1–5 mg  $m^{-2}$ .

On the experimental side, most measurements of an adsorbed amount have concerned adsorption onto colloidal particles, but in that case heterogeneity of the surfaces and aggregation of particles are a considerable concern, and *in situ* measurements of the surface state are generally not possible. Seeking to maximize chemical and topographical homogeneity of the adsorbing solid substrate, we have been working with single solid surfaces instead. In previous work, studying the adsorption onto single solid surfaces of flexible polymers in nonpolar solvents, we established the feasibility of using Fourier transform infrared spectroscopy (FTIR) in the mode of attenuated total reflection (ATR) for studying adsorption of several flexible nonpolar polymers (polystyrene, polymethylmethacrylate, polyisoprene, polydimethylsiloxane, polyethylene oxide) at the single surface of an infrared prism.<sup>10-16</sup> The infrared technique was found to give information not just about the rates of change of aggregate mass

adsorbed, but also about the surface concentration of individual components in the mixture. This study will illustrate the further usefulness of this method to study polymer adsorption from aqueous solution.

The view is often expressed that the main effect on a polyelectrolyte of salt, in an aqueous solution, should be to screen the interaction between charges on the chain. This must certainly play an important role; we show here additional complexity. The complications arise because an aqueous solution is composed of many charged components; a charged polymer competes for access to surface sites with smaller ions. In this study, we address the variables of ionic strength and of surface charge density explicitly. The present paper will describe methods of measurement, the mass adsorbed, and the infrared dichroism when polyelectrolyte chains were allowed to adsorb onto an initially-bare solid surface, and from comparison with a monomeric analogue of the repeat unit along the polyelectrolyte chain we will attempt to estimate the sticking energy. The accompanying paper will consider displacement kinetics when, after one population of chains had become adsorbed to a solid surface of opposite charge, a second population of more strongly charged chains was exposed to this surface to encourage turnover between the adsorbed state and free solution.

## II. EXPERIMENT

### A. Sample cell for ATR

Infrared spectra were collected using a Biorad FTS-60 Fourier transform infrared spectrometer (FTIR) equipped with a broadband mercury cadmium telluride detector. The attenuated total reflection (ATR) optics and the thermostatted homebuilt adsorption cell placed in a nitrogen-purged compartment external to the FTIR spectrometer were described previously.<sup>17</sup> By switching a wire-grid polarizer (Graesby/Specac), spectra in orthogonal *p* and *s* polarizations could be obtained.

The adsorption studies were studied at 25 °C using as substrate a silicon crystal that had been controllably oxidized as described below. The beam was reflected roughly 11 times as it traveled the length of the crystal. The crystal was a rectangular trapezoid of dimensions 50 mm×20 mm×2 mm (Harrick Scientific) whose beam entrance and exit surfaces were cut at 45°. Before each experiment residual polymer was cleaned from the crystal first by UV-ozone treatment for 30 min, followed by ultrasonication in water or ethanol for 15 min. The crystal was then dipped momentarily in 5% HF solution, rinsed copiously in water, and finally treated in UV-ozone plasma cleaner (Harrick Sci. Corp.) for 5 min. The Teflon tubes that served as inlet and outlet conduits to the adsorption cell were cleaned by copious rinsing with water, ethanol, and dried under dry nitrogen. The stainless steel adsorption cell was cleaned by sonication in water or ethanol for 15 min, and then kept in 30% nitric acid for not less than 6 h. It was important to keep the silicon crystal stored under water or ethanol rather than dry. These methods to clean the silicon surface and cell elements and to prepare a reproducible oxide surface are a generalization of methods developed previously for adsorption studies of nonpolar

polymers.<sup>18</sup> The methods have been shown, for experiments in nonpolar solvents, to reproducibly cultivate an oxidized surface (primarily SiO<sub>2</sub> and SiOH) while minimizing the amount of organic contamination from the ambient laboratory. In the present experiments with aqueous media, they yielded adsorption measurements that were quantitatively reproducible from experiment to experiment.

The experiment began after these ministrations. First the cell was filled with D<sub>2</sub>O or aqueous solution, let sit for 1 h for equilibration, and a background spectrum was collected. Polymer solution was not added until 0.5–1 h after the cell had been filled with water or salt solution; this improved the baseline stability.

Interferograms were collected in *p* and *s* polarization with 4 cm<sup>-1</sup> resolution. For static experiments, the number of scans was 512. For dynamic experiments, the number of scans was usually 64 scans during the first 5 min (this took 0.6 min per datum), then 128 scans during the subsequent 10 min (this took 1.2 min per datum), and 512 scans for longer times.

### B. Samples

Poly(1,4vinyl)pyridine (PVP) was selected for study because it is relatively easy to quaternize it to near-completion using well-established methods.<sup>19,20</sup> The parent PVP samples were purchased from Polymer Source, Quebec, Canada. These samples, synthesized by anionic polymerization, were characterized according to manufacturer's specifications by a degree of stereoregularity of 70%. Quaternization was carried out by us in 10 wt. % ethanol solution containing PVP with fivefold excess of ethyl bromide at 60 °C under inert N<sub>2</sub> atmosphere. The reaction was terminated after variable times (after ~15 min, 2 h, or 12 h), to obtain 14%, 48%, or 98% of alkylated pyridine repeat units, by precipitating the polymers into diethyl ether, thus obtaining a family of PVP with a wide range of charge density. In this paper, these polymers are referred to as Q14, Q48, and Q98. Characteristics of the polymers are given in Table I.

The monomer analog of alkylated PVP, the 1,4-dimethylpyridinium cation (P<sup>+</sup>) was purchased from Aldrich (the counterion was iodide, I<sup>-</sup>) and then purified by recrystallization, using precipitation with ethanol, until a clear white color was obtained. Keeping in mind the vulnerability of P<sup>+</sup> to oxidation, experiments were performed soon after recrystallization with care to minimize exposure to light and atmospheric oxygen.

Though it was not feasible to bake the buffer salts, the other inorganic salts (General Storage, pure grade, or Aldrich, purissimum grade) were used as received after control experiments showed no difference if they were baked first at 600 °C to burn out conceivable organic contaminants.

The H<sub>2</sub>O was double-distilled and then further purified by passage through Milli-Q (Millipore) deionizing and filtration columns. Deuterium oxide with 99.9% isotope content was obtained from Cambridge Isotope Laboratories and used without further purification. The results using this solvent were always consistent with those obtained using purified H<sub>2</sub>O, indicating that D<sub>2</sub>O lacked impurities that interfered with the adsorption process. However the amount adsorbed

TABLE I. Characteristics of the electrolyte chains.

Code	Degree of quaternization	$M_w$ (g mol <sup>-1</sup> )	$M_w/M_n^b$	$p_w^b$
Q98	98% <sup>a</sup>	68 000	1.23	325
Q48	48% <sup>a</sup>	52 000	1.23	325
Q14	14% <sup>a</sup>	39 500	1.23	325
Q98-a	98%	54 000	1.15	250

<sup>a</sup>Poly(1,4 vinyl)pyridine was quaternized in our laboratory by alkylation of PVP of  $M_w$  34 000 to variable extents, as described in the text, after purchasing the uncharged polymer from Polymer Sources, Quebec, Canada.

<sup>b</sup> $M_w$  and  $M_n$  denote weight-average and number-average molecular weight, respectively, and  $p_w$  denotes weight-average degree of polymerization.

of  $P^+$  was consistently  $\sim 10\%$  lower in  $D_2O$  than in  $H_2O$ , consistent with known isotope effects<sup>21</sup> (see below). As a matter of terminology, when experiments were performed in  $D_2O$  rather than  $H_2O$ , we will refer to  $pD$  rather than  $pH$ .

### C. Data analysis

The infrared absorption peaks were integrated for purposes of tracking the mass adsorbed. By Beer's Law, both peak height and integration peak intensity would be proportional to polymer concentration, but the latter measure was more reliable in the context of the present experiment since oscillator line shapes might be perturbed by local changes in environment during the course of adsorption. Though deviations from Beer's law are sometimes observed in ATR measurements,<sup>22</sup> this effect originates in changes of the medium's refractive index with absorbent concentration. Changes of this kind were insignificant in the present experiments since the amount of polymer sampled by the ATR signal in dilute aqueous solution was so small. Control experiments, in which the solution concentration was varied systematically, showed Beer's Law to be obeyed; the peak intensity was proportional to the number of oscillators.

The data were analyzed using curve-fitting of the absorption peaks obtained in  $p$  and  $s$  polarizations; the total absorbance was the sum of these values,  $A = A_p + A_s$ . The most consistent results were obtained when 90% of the peaks were assumed to be Gaussian and 10% to be Lorentzian. The peak centers and bandwidths were not fixed, but the results of the curve-fitting were carefully checked for consistency in these parameters. In curve-fitting, a baseline correction was performed to the raw spectra. Note that when the spectra showed large baseline distortion, integration of the peaks gave more consistent results than curve-fitting.

Owing to the large penetration depth of the evanescent wave relative to thickness of the adsorbed layer, the raw measurements in principle included contributions from oscillators in the isotropic polymer solutions in addition to those within the adsorbed polymer layers. This solution contribution was subtracted although its magnitude amounted to only 2% because the solutions were so dilute.

Note that a traditional measure of adsorbed amount refers to the mass of the adsorbate bound to the surface; it is any contribution in excess of that present in the bulk solution and, at the molecular level, it contains contributions from polymer loops, tails, and bound segments. Calibrations of the

mass adsorbed (surface excess) and corrections for the contribution from oscillators in solution are described elsewhere.<sup>17,18</sup> For the silicon crystal that we used, the penetration depth of the evanescent wave was  $0.47 \mu\text{m}$  at  $1643 \text{ cm}^{-1}$ . The calibrated contribution of PVP in solution gave, for the sum of absorbance in  $s$  and  $p$  polarization, the effective extinction coefficient of  $0.0066$  absorbance units per  $\text{mg mL}^{-1}$  ( $1.4$  absorbance units per molar concentration unit) of  $N$ -ethyl-pyridinium bromide rings ( $1643 \text{ cm}^{-1}$  band) and  $0.008$  absorbance units per  $\text{mg mL}^{-1}$  ( $0.83$  absorbance units per molar concentration unit) of uncharged pyridine rings ( $1604 \text{ cm}^{-1}$  band) in the PVP molecules. From these numbers and the known value of penetration depth and composition of the PVP molecules, the calibration constants to calculate the adsorbed amounts were obtained. As an example, for the  $1643 \text{ cm}^{-1}$  band, these values were  $0.028 \text{ abs units m}^2 \text{ mg}^{-1}$  for Q98 and  $0.031 \text{ abs units m}^2 \text{ mg}^{-1}$  for Q48. Note that twice as big extinction coefficients were found for the monomer analog of PVP,  $P^+$ , possibly due to the minor difference in the molecular structure and the different counterion ( $I^-$  instead of  $Br^-$  for PVP). The calibrations of solution contribution (roughly 25% of the total signal for a solution concentration of  $1 \text{ mg mL}^{-1}$  and proportionately less with lower solution concentration) were verified to be the same in  $H_2O$ ,  $D_2O$ , and salt solutions up to  $0.5 \text{ M NaCl}$ . This calibration contribution from chains free in solution was subtracted quantitatively from all of the measurements presented below.

Dichroic ratio,  $D$ , was defined as the ratio of infrared absorption in  $p$  and  $s$  polarization directions. Considering the polymer solution to be an isotropic medium with the refractive index of water ( $1.33$ ) and the known refractive index of silicon ( $3.42$ ), straightforward calculation<sup>23,24</sup> shows that  $D = 2.05$  indicates isotropy.

The spectra were examined at each stage of the experiments for infrared bands indicating the presence of contaminating surface species, and the experiment was aborted if contamination was encountered.

## III. RESULTS AND DISCUSSION

This paper concerns PVP adsorption onto an initially-bare surface of oxidized silicon, and the accompanying paper concerns the sequential adsorption of more highly-charged chains onto a surface whose coverage had previously been saturated by chains with lesser charge density.

### A. Representative spectra

To reduce overlap of the infrared spectra of PVP with those of water itself, we often dissolved the polymer in  $D_2O$  rather than  $H_2O$ , as noted in the Experiment. The measurements of adsorption at variable  $pH$  were performed in  $H_2O$  but all others in this paper were performed in  $D_2O$ . As already noted in  $D_2O$  the amount adsorbed was  $\sim 10\%$  less at a given  $pH$ , probably because of the known isotopic influence on the dissociation constant of surface silanol groups,<sup>21</sup> but we verified that the main results presented below did not depend on the choice of  $H_2O$  or  $D_2O$  solvent.

Figure 1 shows ATR spectra recorded for partially-alkylated PVP, Q48, in  $D_2O$ . Absorbance in the infrared re-

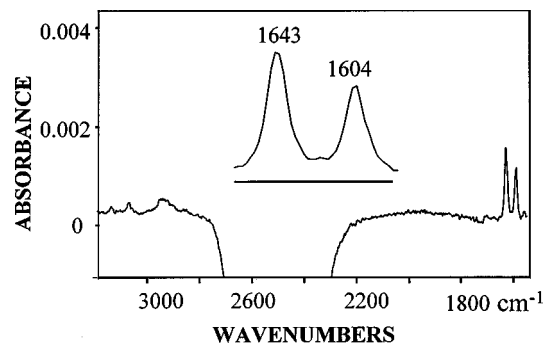


FIG. 1. Absorbance plotted against wave number in the infrared spectrum for 48% quaternized poly(1,4 vinyl)pyridine (Q48) adsorbed onto oxidized silicon from  $D_2O$  at  $pD=9.2$ . The measurements were made in the FTIR-ATR mode. Since the spectrum in the presence of adsorbed Q48 was ratioed to the spectrum of  $D_2O$  in pure buffer solution, the intense negative  $D_2O$  band (centered at  $2480\text{--}2500\text{ cm}^{-1}$ ) reflects displacement of  $D_2O$  from the near-surface region to accommodate positive adsorption of the polymer. Among the polymer bands, the aliphatic and aromatic C–H stretches (centered at  $2864$  and  $2940\text{ cm}^{-1}$  and just above  $3000\text{ cm}^{-1}$ , respectively) are weak and poorly resolved. The pyridine ring bands (centered at  $1604\text{ cm}^{-1}$  for the neutral pyridine ring but at  $1643\text{ cm}^{-1}$  for the quaternized ring) are magnified in the inset. These were used to determine the degree of quaternization and the adsorbed amount.

gion is plotted against wave number. Most prominent was the intense negative absorption from  $D_2O$ , indicating that heavy water was displaced from the near-surface region as PVP was adsorbed; its strong intensity reflects strong infrared absorptivity of  $D_2O$ . The  $D_2O$  negative peak did not overlap with PVP absorption, however. In Fig. 1, one notices the carbon-hydrogen vibrations (along the chain backbone and in the pyridine ring), located in the neighborhood of  $3000\text{ m}^{-1}$ ; their intensity was so low that they were difficult to resolve. We do not consider them further because the skeletal in-plane vibrations of the pyridine ring provided similar information with a higher ratio of signal to noise. These vibrations, shown magnified in the inset, were centered at  $1604\text{ cm}^{-1}$  for the neutral ring and at  $1643\text{ cm}^{-1}$  for the charged (quaternized) ring. Protonation of the pyridine ring was not an issue because the  $pD$  was high, much higher than the  $pK$  ( $pK\sim 5\text{--}5.5$ ) to protonate the pyridine ring through acid–base equilibrium. Therefore we attribute all intensity of the  $1643\text{ cm}^{-1}$  band to permanent charge.

Control experiments showed also that the spectra obtained in the ATR experiments were the same as obtained in transmission. Hence, in the analysis presented below, adsorption of the pyridine and pyridinium rings was used to determine the degree of quaternization and the adsorbed amount. To calculate the fraction of quaternized units, we used the ratio of the molar extinction coefficients of 1,4(vinyl)pyridine rings, quaternized or not quaternized by ethyl bromide, which is known to be 1.68.<sup>25</sup>

## B. Adsorption kinetics

Figure 2 illustrates the kinetics of Q98a adsorption at a concentration much lower than in the further experiments presented below. Mass adsorbed [Fig. 2(a)] and dichroism of the pyridinium ring [Fig. 2(b)] are plotted against elapsed time. Both quantities reached a near-steady state after  $\sim 1$  h.

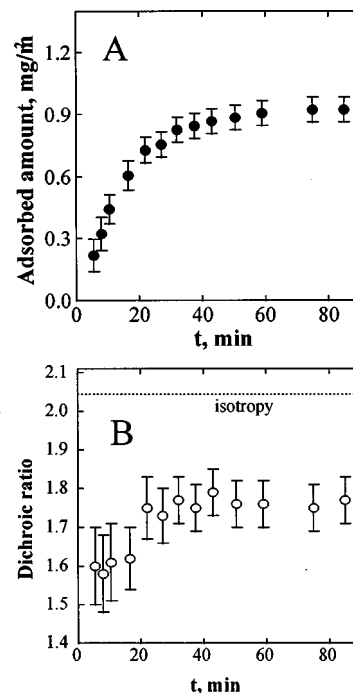


FIG. 2. Mass adsorbed (a) and infrared dichroism of the pyridinium ring,  $D$  (b) plotted against elapsed time for adsorption of Q98-a ( $0.005\text{ mg mL}^{-1}$ ,  $0.1\text{ M NaCl}$ ,  $pD=9.2$ ) onto an initially-bare surface of oxidized silicon.

Very slow subsequent growth in the mass adsorbed, 2%–3% per day, could also be detected at longer times. It is interesting to notice that this slow long-time equilibration is reminiscent of effects also seen for the adsorption of nonpolar polymers.<sup>26</sup> It is also interesting to notice the anisotropy of the pyridinium rings at this salt concentration,  $0.1\text{ M}$  (see additional experiments presented below). The observed slight increase in the average dichroism of pyridinium rings with increased adsorption time is consistent with more “random” polymer conformation in the denser adsorbed layer.

However, the adsorption of polymer from higher concentrations was more rapid. These systems were quick to reach steady-state mass adsorbed—in stark contrast to what transpired (see accompanying paper) in the course of adsorption onto previously-adsorbed polymer.

## C. Demonstration that adsorption proceeded by electrostatic attraction

The isoelectric point of oxidized silicon is expected to be close to that of amorphous silica; for this, values of 3.0,<sup>27</sup> 3.42,<sup>28</sup> or even 2.0 (Ref. 29) have been reported. The surface charge density was thus negative at  $pH>3\text{--}4$  and it increased with increasing  $pH$ . Quantitative estimates of the  $pH$  dependence of the surface charge are readily calculated from the reported  $pK_a=9.2$ , as sketched in Fig. 3(b). The maximum charge density of ionized SiOH on a silica surface has been reported to be in the neighborhood of  $20\text{ \AA}^2\text{--}25\text{ \AA}^2$  per surface  $SiO^-$  group.<sup>30</sup>

Experiments were performed in which polymers Q48 and Q98a were allowed to adsorb from  $H_2O$  at variable  $pH$  with no salt added except as needed to produce the buffer solution at a given  $pH$ . The large increase of the mass ad-

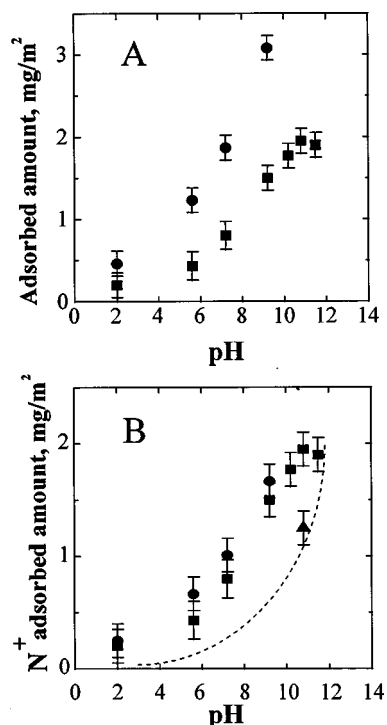


FIG. 3. Total mass adsorbed (a) and mass adsorbed of pyridinium segments (b) plotted against  $pH$  for Q14 (triangles), Q48 (circles), and Q98-a (squares) after adsorption to initially-bare oxidized silicon. No salt was added except as needed to produce the buffers with the given  $pH$ . The compositions of the buffer solutions were 0.01 M HCl ( $pH=2$ ), 2 mM mixtures of  $Na_2HPO_4$  and  $NaH_2PO_4 \cdot H_2O$  ( $pH=5.6$  and  $pH=7.3$ ), 2 mM  $Na_2B_4O_7 \cdot 10H_2O$  ( $pH=9.2$ ), 2 mM  $Na_2CO_3$  ( $pH=10.5$ ), and 2 mM  $Na_2CO_3$  and some amount of NaOH as needed to increase  $pH$  ( $pH=11.5$ ). The dashed line in (b) estimates the  $pH$  dependence of the surface charge on silica; the expected charge density of the bare surface, calculated from the  $pK \approx 9.2$  for silica, is plotted against  $pH$  on a linear scale with arbitrary units. It is evident that the anticipated surface charge on the bare surface increased more slowly than the adsorption of charged polymer.

sorbed with increasing  $pH$  [Fig. 3(a)]—by a factor of nearly 10 as the surface charge density was increased with increase of  $pH$ —is attributed to heightened electrostatic attraction between the PVP chains and the silicon surface of opposite charge. It is also true that we also observed a small residual adsorption at  $pH=2$ , when the silicon surface should be positively charged or neutral, possibly showing the small residual influence of weaker polarization attractions.

The main point is that the mass adsorbed of Q48 at a given  $pH$  was nearly twice as large as for Q98a. It thus became relevant to normalize the mass adsorbed by the degree of quaternization. Figure 3(b) shows that the mass adsorbed of charged units, the pyridinium units of PVP, was sensibly independent of the degree of quaternization. The relevant variable, in determining the amount adsorbed, appears to have been charge density on the adsorbing chain.

An additional point of interest is that charge of the adsorbed polymer molecules was always, except at the highest  $pH$ , considerably higher than the charge on the native surface of oxidized silicon. The dashed line in Fig. 3(b) shows the expected charge density of the bare surface, calculated from the  $pK \approx 9.2$  for silica.<sup>31</sup> It is considerably less than the

areal density of adsorbed pyridinium groups, also shown in Fig. 3(b).

Why did the mass of electrostatically-adsorbed polymer increase with  $pH$  (roughly in linear proportion to  $pH$ ) with magnitude so much larger than the expected charge density on the bare surface itself? The first possibility to consider is the known switch in the sign of the net surface charge after adsorption of oppositely charged polyelectrolytes, owing to excess charge carried to the surface in loops and tails,<sup>32,33</sup> but this effect is too small to explain alone the observed twofold discrepancy in charge at intermediate  $pH$  ( $pH \approx 4-10$ ). A more plausible explanation is that when polyelectrolyte adsorbs it induces additional ionization of the underlying surface. This was experimentally measured by several authors, including one of us.<sup>29,34,35</sup>

#### D. Effects of varying the salt concentration

The remainder of the experiments in this study were performed at  $pD=9.2$  and  $10.5$ —conditions of high surface charge density, where the amount of Q98 adsorbed showed minimal dependence on  $pD$ . The reported  $pK_a \approx 9.1-9.4$  of the isolated SiOH group<sup>31</sup> (note that this number appears to be further decreased by proximity of other SiOH groups at a surface<sup>36</sup>) implies that, at  $pD=9.2$ ,  $\approx 50\%$  of the silanol surface groups on the bare surface were dissociated when the salt concentration was low. This may be compared to the estimated mean area of  $20-25 \text{ \AA}^2$  expected for Si-OH groups on silica.<sup>30</sup>

It was predicted some time ago that the amount of polyelectrolyte adsorbed should increase with ionic strength to the point of a maximum, beyond which it decreases.<sup>5,6</sup> To test this view for the present system, experiments were performed in which the salt concentration was varied by adding either NaCl or KI to the buffer solution. Both are simple monovalent species, yet reflection showed that two distinctively different types of effects might be expected. First, the cations,  $Na^+$  and  $K^+$ , would compete with the polyelectrolyte for access to the surface; this is the effect that has been considered theoretically.<sup>37</sup> Secondly, the anions,  $Cl^-$  and  $I^-$ , would compete with the negatively-charged surface for association with the polyelectrolyte; this might influence solubility of the polyelectrolyte in bulk solution. The second effect might be particularly likely when one considers that from a decrease of the critical micelle concentration (cmc) of 1-methyl-4-alkylpyridinium salts, affinity of halogen ions for the pyridinium ring is thought to vary in the order  $I^- > Br^- > Cl^-$ .<sup>38</sup>

In fact, both effects were observed. Figure 4(a) compares the mass adsorbed from NaCl and KI. In the presence of both salts the amount adsorbed doubled as the salt concentration was increased from a low level, but for KI salt a point of actual bulk insolubility was reached at a low concentration,  $[I^-]=0.05 \text{ M}$ . For NaCl this did not happen and the polyelectrolyte remained soluble at salt concentrations in excess of 4 M. The prominence of chemically-specific interactions is emphasized by this observation. Counterions, even monovalent counterions, may interact with a polyelectrolyte in fashions much more complex and chemically-specific than

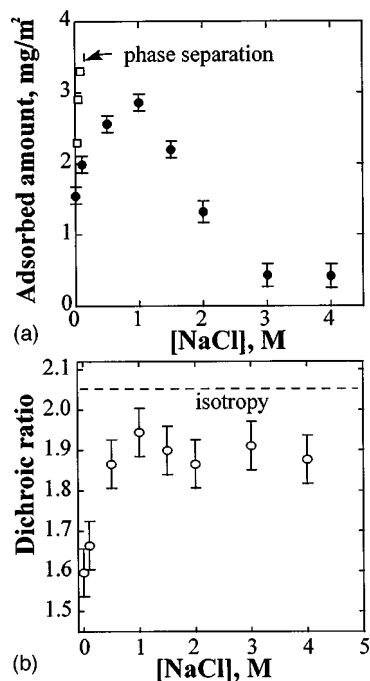


FIG. 4. Mass adsorbed (a) and dichroic ratio,  $D$  (b) of Q98-a ( $1 \text{ mg mL}^{-1}$ ) adsorbed onto an initially-bare surface of oxidized silicon at  $pD=9.2$ . With ionic strength controlled by KI (squares) the mass adsorbed grew with increasing salt concentration and this was terminated by phase separation of the bulk solution at  $0.050 \text{ M}$  KI. In (a) the datum at highest mass adsorbed refers to  $0.045 \text{ M}$  KI. With ionic strength controlled by NaCl (circles) the mass adsorbed showed a maximum with increasing salt concentration. In (b) the dashed line at  $D=2.05$  indicates isotropic orientation.

would be predicted just from considering them as point charges as in a Debye–Hückel-type approach.

It is particularly provocative that the maximum mass adsorbed occurred at very high ionic strength ( $1 \text{ molar NaCl}$ ). A reasonable interpretation<sup>6</sup> is that it was a consequence of specific interactions of polyelectrolyte segments and  $\text{Na}^+$  ions with the surface. The polyelectrolyte adsorbed from low salt concentration relatively flat, but increasing salt concentration saw more and more competitive adsorption of  $\text{Na}^+$  with the polymer charged segments for access to surface sites on the silicon surface. The polymer then rearranged to conformations with a greater abundance of loops and tails. This led to more extended layers<sup>8,39–43</sup> and in this process the amount adsorbed doubled. Parenthetically, we note that since ionization of surface silanol groups rises with increased concentration of salt. This also contributed to the measured increase in the adsorbed amount but this effect is secondary in importance; it can explain only 20% rise of the amount adsorbed in contrast to the doubling observed in the experiment. (Also, using completely ionized mica as a substrate, we have confirmed in parallel experiments that thicker polyelectrolyte layers formed at this  $pH$  at these high salt concentrations.<sup>44</sup>) At still higher salt concentrations, one sees in Fig. 4(a) that the  $\text{Na}^+$  actually began to displace the polyelectrolyte from the surface. At the highest concentrations of  $\text{Na}^+$  studied, displacement of the polyelectrolyte was virtually complete. A similar observation was made by Cohen Stuart and co-workers on a different polyelectrolyte system<sup>29,45</sup> and confirms the generality of the effect.

## E. Dichroism of adsorbed pyridinium rings

It also emerged that the pyridinium rings of the polyelectrolyte repeat unit became adsorbed with a definite mean surface orientation. To quantify surface orientation, we calculated the dichroic ratio ( $D$ ), defined in Sec. II. While  $D$  in this experiment was probably slightly influenced by residual roughness of the polished Si crystals, it is meaningful to compare relative values of  $D$  measured using the same crystal under different solution conditions. We analyzed  $D$  of the carbon–nitrogen stretch at  $1643 \text{ cm}^{-1}$ , an in-plane stretch. This band is believed to be directed along the symmetry axis of the ring and should reflect the segmental tilt.

Figure 4(b) shows the dependence of the dichroic ratio on the salt concentration ( $\text{NaCl}$ ). In “low salt” conditions (adsorption from the buffer alone), the pyridinium rings adsorbed preferentially parallel to the surface, but the dichroic ratio increased monotonically with increasing salt concentration until reaching a plateau at which the mean segmental orientation was nearly isotropic. The near-isotropy is consistent with the looser, fluffier layer that was implied in Fig. 4(a) by the enhanced amount adsorbed; it is reasonable to think that pyridinium rings in physical contact with the surface remained relatively flattened while pyridinium rings that dangled into solution were isotropic or nearly so. It is notable that the maximum mass adsorbed and the plateau dichroic ratio were achieved at the same (high) salt concentration.

Parenthetically, it is worth remarking that dichroism must also depend on a chain’s stereoregularity. If a chain is atactic, and a given pyridine ring is adsorbed preferentially parallel to the surface, it is not geometrically possible for adjoining rings also to lie parallel, owing to the irregular spatial positioning of the pyridine rings pendant to the chain backbone. Indeed, in a control experiment we found that a PVP polymer obtained by free radical polymerization (and therefore expected to be atactic) did not display significant infrared anisotropy in the pyridine ring. It is interesting to conclude that the mode of charge–surface interaction, as the charged polyelectrolyte interacts with a surface of opposite charge, therefore depends subtly on details of stereoregularity along the polyelectrolyte backbone.

## F. Segmental sticking energy of the PVP repeat unit

In this section, we attempt to quantify the competitive strength of the adsorption of  $\text{Na}^+$  ions and polyelectrolyte segments. The organic monomer molecule, the 1,4-dimethylpyridinium cation ( $\text{P}^+$ ), was selected as the segmental analogue of alkylated poly(1,4-vinylpyridine). Figure 5 shows the surface excess of  $\text{P}^+$  plotted as a function of its solution concentration at “low” and “high”  $\text{NaCl}$  salt concentrations. This adsorption isotherm reflects the competitive adsorption of  $\text{Na}^+$  and  $\text{P}^+$ .

An estimate of the sticking energy of  $\text{P}^+$ , relative to  $\text{Na}^+$ , follows from the classical Langmuir isotherm (we discuss below the reasonability of its assumptions). In the framework of this model and for a two-component system with species  $A$  and  $B$ , one has the well-known relation,

$$\theta_A = K_A X_A / (K_B X_B + K_A X_A), \quad (1)$$

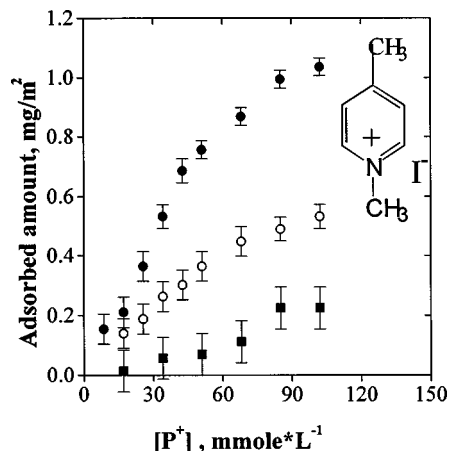


FIG. 5. Mass adsorbed of a monomer analog of the polyelectrolyte charged repeat unit, the 1,4-dimethylpyridine ( $P^+$ ) ion, adsorbed onto an initially-bare surface of oxidized silicon at  $pH=9.2$ , plotted against its solution concentration. Adsorption was measured in the presence of 3 mM buffer (filled circles), 0.03 M NaCl (open circles), and 0.5 M NaCl (squares).

where  $\theta$  is the fractional surface coverage,  $X$  are mole fractions, and  $K$  are equilibrium constants for the adsorption of species  $A$  and  $B$  in the absence of the other component. Using the data in Fig. 5, Fig. 6 shows a plot of  $1/\theta_{P^+}$  as a function of  $1/X_{P^+}$ . We omit high surface coverages, which should not be expected to fit (and do not fit) the linear relation implied by Eq. (1). At low surface coverages the slope is  $1/K_{\text{eff}} = K_{\text{Na}^+} X_{\text{Na}^+} / K_{P^+}$ .

The effective sticking energy,  $\Delta h_{\text{eff}}$ , expressing the surface affinity of  $P^+$  relative to  $\text{Na}^+$ , can now be estimated using the relation

$$K_{\text{eff}} = \exp(\Delta h_{\text{eff}} / k_B T), \quad (2)$$

where  $k_B$  is the Boltzmann constant and  $T$  is the absolute temperature. Expressed in units of thermal energy  $k_B T$ , this gives  $\Delta h_{\text{eff}} \approx 7k_B T$  (buffer solution) and  $4.5k_B T$  (0.5 M NaCl). In common with  $\chi_s$ , the well-known dimensionless free energy needed for replacement of an adsorbed solvent molecule by a chain segment,<sup>37</sup> this estimate of  $\Delta h_{\text{eff}}$  expresses relative surface affinity.

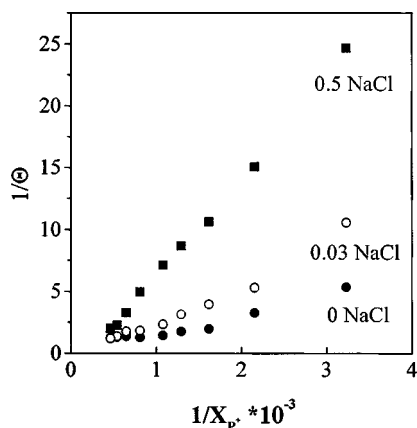


FIG. 6. Inverse fractional surface coverage,  $1/\theta$ , plotted against inverse molar solution fraction of  $P^+$ ,  $1/X_{P^+}$ . By Eq. (2), the slope provides an estimate of the sticking energy. Symbols are the same as in Fig. 5.

These estimates are comparable to the strength of a hydrogen bond. This order of magnitude is plausible though the number itself is certainly tentative given the simple model on which it is predicated. Since the active variable is the ratio of mole fractions of  $P^+$  and  $\text{Na}^+$ , use of Eq. (1) amounts to assuming that the activity coefficient is proportional, for  $P^+$  and  $\text{Na}^+$ , to the mole fraction by the same constant of proportionality. Apart from this (the strongest) assumption, the assumptions of single site-adsorbate interactions and of the absence of lateral interactions should be relatively robust when the surface coverage is low. To put the magnitude of  $\Delta h_{\text{eff}}$  into perspective, the energetic attraction of  $\text{Na}^+$  and  $\text{Cl}^-$ , if they could be spaced in vacuum at a separation equal to the sum of their hydrated radii, would be  $80k_B T$  at room temperature, and this would be reduced in water by a factor equal to dielectric constant for 2 charges in close proximity. The precise magnitude will depend sensitively on issues that are so poorly understood that it is impossible to obtain reliable estimates; the effective dielectric constant, changes in the hydrated radius when two charged groups come into close proximity, the relevant hydrated radius of an organic ion with complex shape (such as  $P^+$ ), and the well-known subtleties of ion-ion correlations.<sup>46</sup> From the raw data in Fig. 5, it is obvious that  $P^+$  and  $\text{Na}^+$  have similar surface affinity (if not, they would not compete successfully for access to the same surface sites).

The effect of ionic strength on the adsorbed polyelectrolyte appears then to be not only to screen charges; it is also to disrupt the intensity of surface-segment bonds. Specifically, increasing the ionic strength appears to have the effect of lowering the effective sticking energy of segments along the adsorbing polymer. If our tentative estimate of the sticking energy is correct, the magnitude appears to exceed the weak-adsorption limit in which facile equilibration of the adsorbed layer should be expected.

The following paper<sup>47</sup> explores consequences of electrostatic adsorption for exchange reactions when chains of one type are allowed to adsorb initially and then chains with a larger propensity to adsorb are introduced into the bulk solution. Keeping in mind the conclusions just stated, it will not be surprising to find the occurrence of trapped, metastable states.

## ACKNOWLEDGMENTS

We are indebted to Alexander D. Schwab for performing, as an undergraduate summer researcher, the experiments that involved Q14. This research was supported by donations from the Exxon Research and Engineering Corp., the International Fine Particle Research Institute (IFPRI), and by the taxpayers of the United States through the National Science Foundation.

<sup>1</sup>F. Th. Hesslink, *J. Colloid Interface Sci.* **60**, 448 (1977).

<sup>2</sup>M. Muthukumar, *J. Chem. Phys.* **86**, 7230 (1987).

<sup>3</sup>O. V. Borisov, E. B. Zhulina, and T. M. Birshtein, *J. Phys. II* **4**, 913 (1994).

<sup>4</sup>V. Shubin and P. Linse, *J. Phys. Chem.* **99**, 1285 (1995).

<sup>5</sup>M. R. Böhmer, O. A. Evers, and J. M. H. M. Scheutjens, *Macromolecules* **23**, 2288 (1990).

- <sup>6</sup>H. G. M. van de Steeg, M. A. Cohen Stuart, A. de Keizer, and B. H. Bijstebosch, *Langmuir* **8**, 2538 (1992).
- <sup>7</sup>P. Linse, *Macromolecules* **29**, 326 (1996).
- <sup>8</sup>M. A. Cohen Stuart, G. J. Fleer, J. Lyklema, W. Norde, and J. M. H. M. Scheutjens, *Adv. Colloid Interface Sci.* **34**, 477 (1991).
- <sup>9</sup>G. J. Fleer, M. A. Cohen Stuart, J. M. H. M. Scheutjens, T. Cosgrove, and B. Vincent, *Polymers at Interfaces* (Chapman & Hall, London, 1993), p. 502.
- <sup>10</sup>H. E. Johnson and S. Granick, *Science* **255**, 966 (1992).
- <sup>11</sup>J. F. Douglas, H. E. Johnson, and S. Granick, *Science* **262**, 2010 (1993).
- <sup>12</sup>P. Frantz and S. Granick, *Macromolecules* **27**, 2553 (1994).
- <sup>13</sup>P. Frantz and S. Granick, *Macromolecules* **28**, 6915 (1995).
- <sup>14</sup>H. M. Schneider, P. Frantz, and S. Granick, *Langmuir* **12**, 994 (1996).
- <sup>15</sup>E. P. Enriquez and S. Granick, *Colloids Surf., A* **113**, 11 (1996).
- <sup>16</sup>I. Soga and S. Granick, *Macromolecules* **31**, 5450 (1998).
- <sup>17</sup>P. Frantz and S. Granick, *Macromolecules* **28**, 6915 (1995).
- <sup>18</sup>P. Frantz and S. Granick, *Langmuir* **8**, 1176 (1992).
- <sup>19</sup>R. M. Fuoss and U. P. Strauss, *J. Polym. Sci.* **3**, 246 (1948).
- <sup>20</sup>A. L. Margolin, V. A. Izumrudov, V. K. Švedas, A. B. Zezin, V. A. Kabanov, and I. V. Berezin, *Biochim. Biophys. Acta* **660**, 359 (1981).
- <sup>21</sup>P. K. Glasoe and F. A. Long, *J. Phys. Chem.* **64**, 188 (1960).
- <sup>22</sup>N. J. Harrick and K. H. Beckmann, in *Characterization of Solid Surfaces*, edited by P. F. Kane and G. B. Larrabee (Plenum, New York, 1974).
- <sup>23</sup>S. Frey and L. K. Tamm, *Biophys. J.* **60**, 922 (1991).
- <sup>24</sup>R. P. Sperline, Y. Song, and H. Freiser, *Langmuir* **8**, 2183 (1992).
- <sup>25</sup>Prof. V. Izumrudov, Moscow State University, Department of Polymer Chemistry (private communication).
- <sup>26</sup>H. E. Johnson and S. Granick, *Macromolecules* **23**, 3367 (1990).
- <sup>27</sup>G. A. Parks, *Chem. Rev.* **65**, 177 (1964).
- <sup>28</sup>E. Kokufuta and K. Takahashi, *Macromolecules* **19**, 351 (1986).
- <sup>29</sup>N. G. Hoogeveen, M. A. Cohen Stuart, and G. J. Fleer, *J. Colloid Interface Sci.* **182**, 133 (1996).
- <sup>30</sup>R. K. Iler, *Chemistry of Silica* (Wiley, New York, 1979).
- <sup>31</sup>D. D. Perrin, *Ionization Constants of Inorganic Acids and Bases in Aqueous Solution* (Pergamon, New York, 1982), p. 99.
- <sup>32</sup>I. D. Robb and M. Sharples, *J. Colloid Interface Sci.* **89**, 301 (1982).
- <sup>33</sup>P. A. Williams, R. Harrop, G. O. Phillips, I. D. Robb, and G. Pass, in *The Effect of Polymers on Dispersion Properties*, edited by Th. F. Tadros (Academic, London, 1982), p. 361.
- <sup>34</sup>B. C. Bonekamp and J. Lyklema, *J. Colloid Interface Sci.* **113**, 67 (1986).
- <sup>35</sup>S. A. Sukhishvili, O. S. Chechik, and A. A. Yaroslavov, *J. Colloid Interface Sci.* **178**, 42 (1996).
- <sup>36</sup>E. Kokufuta, S. Fujii, Y. Hirai, and I. Nakamura, *Polymer* **23**, 452 (1982).
- <sup>37</sup>G. J. Fleer, M. A. Cohen Stuart, J. M. H. M. Scheutjens, T. Cosgrove, and B. Vincent, *Polymers at Interfaces* (Chapman & Hall, London, 1993).
- <sup>38</sup>E. J. R. Sudholter and J. B. N. Engberts, *J. Phys. Chem.* **83**, 1854 (1982).
- <sup>39</sup>M. C. Café and I. D. Robb, *J. Colloid Interface Sci.* **86**, 411 (1982).
- <sup>40</sup>J. Meadows, P. A. Williams, M. J. Garvey, R. A. Harrop, and G. O. Phillips, *Colloids Surf., A* **32**, 275 (1988).
- <sup>41</sup>V. Shubin and P. Linse, *J. Phys. Chem.* **99**, 1285 (1996).
- <sup>42</sup>H. A. van der Schee and J. Lyklema, *J. Phys. Chem.* **88**, 6661 (1984).
- <sup>43</sup>B. C. Bonekamp, H. A. van der Schee, and J. Lyklema, *Croat. Chem. Acta* **56**, 695 (1983).
- <sup>44</sup>S. A. Sukhishvili, A. Dhinojwala, and S. Granick (submitted).
- <sup>45</sup>B. C. Bonekamp, Ph.D. thesis, Wageningen Agricultural University, The Netherlands, 1984, as quoted in Ref. 8.
- <sup>46</sup>R. Kjellander, S. Marčelja, R. M. Pashley, and J. P. Quirk, *J. Chem. Phys.* **92**, 4399 (1990).
- <sup>47</sup>S. A. Sukhishvili and S. Granick, *J. Chem. Phys.* **109**, 6869 (1998), following paper.